SOILS AND FOUNDATIONS Vol. 42, No. 4, 29-41, August 2002
Japanese Geotechnical Society

USE OF COMPRESSIBLE EXPANDED POLYSTYRENE BLOCKS AND GEOGRIDS FOR RETAINING WALL STRUCTURES

YOSHIMICHI TSUKAMOTO[i], KENJI ISHIHARA[ii], HIROHITO KON[iii] and TAKAYUKI MASUO[iv]

ABSTRACT

The use of a compressible layer such as expanded polystyrene blocks behind a rigid retaining wall and geogrid layers embedded in a dense granular backfill is examined as a reinforcement technique for retaining wall structures. The mobile model retaining walls adjacent to reinforced model specimens are subjected to different surcharge pressures, and are caused to move laterally to measure the lateral earth pressure during the wall movement. The coefficients of earth pressure at rest and active earth pressure are carefully inferred from test results. Three series of tests are conducted; one test series with expanded polystyrene blocks installed behind the wall, another with geogrid layers embedded within model specimens, and the last series with expanded polystyrene blocks installed behind the wall and geogrid layers fixed between two adjacent expanded polystyrene blocks and embedded within model specimens. The reductions in the earth pressure at rest and the active earth pressure due to various patterns of reinforcement are interpreted in relation to the concept of controlled yielding of compressible expanded polystyrene blocks, tensile strains induced along geogrid layers, fixity between expanded polystyrene blocks and geogrid layers, and a facing unit consisting of expanded polystyrene blocks.

Key words: active earth pressure, earth pressure, earth pressure at rest, (EPS), (geogrids), model test, retaining wall, sandy soil (**IGC**: E5/H2)

INTRODUCTION

Lightweight expanded polystyrene (EPS) blocks have become widely used to improve the stability of earth structures in a variety of manners. They are employed for instance to improve the bearing capacity of soft soil foundations for the construction of embankments and temporary roads, to increase the stability of retaining wall structures and steep slopes, and to eliminate overburden pressures on underground structures when installed as backfill materials.

In retaining wall structures, reinforcement by means of geogrids is frequently employed. They are installed in several layers within backfill materials, and are sometimes tied or untied to the wall structures. It has also become known that the inclusion of a compressible geosynthetic layer immediately behind a rigid retaining wall leads to the reduction of lateral earth pressure, whereby the retaining wall structure can gain more internal stability. This construction technique was successfully employed in the field and reported by Partos and Kazaniwsky (1987) among others, in which a prefabricated expanded polystyrene bead drainage board was used for the construction of a 10 metres high basement wall. Karpurapu and Bathurst (1992) examined the effects of a compressible layer behind a rigid wall on lateral earth pressure by employing an FEM analysis, and the concept of controlled yielding was introduced. Suppose the retaining wall structure comprising a rigid wall and a compressible geosynthetic layer is subjected to lateral earth pressures from backfill materials, while the rigid wall is kept stationary. Earth pressure causes lateral compression of the geosynthetic layer. However, the soil behind the wall structure is in turn subjected to lateral expansion in proportion to the lateral compression of the geosynthetic layer, and therefore is caused to deform plastically towards an active stress state condition. This phenomenon is characterized by the interference between the increase in the compressive stress on the geosythetic layer and the reduction in the lateral earth pressure exerted by the soil.

In this study, multiple series of tests are carried out on model retaining walls with compressible expanded polystyrene blocks installed immediately behind the walls, on walls with geogrid layers embedded within backfills but not tied to the walls, and on walls reinforced not only with expanded polystyrene blocks but also with geogrid layers.

[i] Lecturer, Department of Civil Engineering, Tokyo University of Science, Japan.
[ii] Professor, ditto.
[iii] Geotop Corporation, Japan (Formerly Graduate Student, Department of Civil Engineering, Tokyo University of Science, Japan).
[iv] Taiyo Kogyo Corporation, Japan.
Manuscript was received for review on April 16, 2001.
Written discussions on this paper should be submitted before March 1, 2003 to the Japanese Geotechnical Society, Sugayama Bldg. 4F, Kanda Awaji-cho 2-23, Chiyoda-ku, Tokyo 101-0063, Japan. Upon request the closing date may be extended one month.

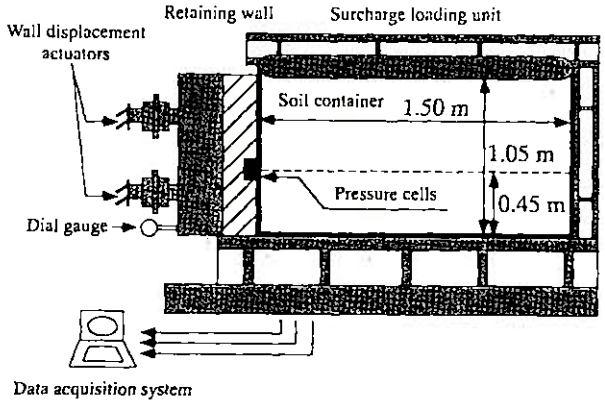

Fig. 1. Test apparatus

EXPERIMENTAL DETAILS

Test Apparatus

Figure 1 shows the elevation and plan views of the test apparatus used in this study. This apparatus is made up of a model soil container, a mobile model retaining wall, wall displacement actuators, a surcharge loading unit, and a data acquisition system.

The model soil container is 1.5 m in width, 1.5 m in length and 1.05 m in height. All the model specimens including expanded polystyrene blocks and geogrid layers are prepared in this container. One of the walls located at the front, 1.5 m in width and 1.05 m in height, constitutes a mobile retaining wall motor-driven by the four combinations of motor and actuator units, by which to produce a smooth translational horizontal displacement of the wall. Herein, the translational displacement represents a wall movement with the orientation of the wall always standing perpendicular to the floor. On the mobile retaining wall located 0.3 m apart and 0.45 m above the floor are two pressure cells, by which to measure lateral earth pressures on the mobile retaining wall. The face of the pressure cells is 85 mm in diameter. These pressure cells are capable of measuring a pressure of up to 980 kPa, and constitute a diaphragm on which strain gauges are attached. The lateral earth pressure reported in this study is calculated as the average reading of these two pressure cells, and the wall displacement is measured by a dial gauge attached to the mobile retaining wall. On top of the model soil container is a surcharge-loading unit consisting of an inflatable rubber mattress and a rigid lid. When the model specimen is prepared in the model container, the rubber mattress is installed on the top surface of the model specimen, and the model container is closed by tightly fixing the rigid lid to it. The rubber mattress is then air-inflated using the unit of an air-compressor and a regulator located outside of the model container, and produces a surcharge pressure on the model specimen. All the voltage outputs from the pressure cells, the dial gauge, and the strain gauges for geogrid layers are recorded and stored in data files on a personal computer.

Table 1. Material properties of geogrids

	Type A	Type B
Polymer type	Vinylon	Vinylon
Mass/unit area (g/m^2)	320	200
Aperture size, L (mm) × W (mm)	16 × 16	19 × 16
Secant tensile stiffness at 1.0% strain (kN/m)	1300	560
Strain at failure, ε_f (%) (at 1%/minute)	9	10
Rupture strength (kN/m)	58.8	29.4

Soil and Reinforcement Materials

In this study, one granular soil, one type of expanded polystyrene material, and two types of geogrids are used to prepare model specimens.

Toyoura sand is used as a model granular backfill in this study, which is classified as poorly graded clean fine sand with no fines of less than 0.075 mm particle diameter. The physical properties of this sand are as follows; specific gravity $G_s = 2.65$, mean particle diameter $D_{50} = 0.19$ mm, uniformity coefficient $U_c = 1.70$, maximum void ratio $e_{max} = 0.988$, minimum void ratio $e_{min} = 0.616$.

In industrial applications, a variety of types of expanded polystyrene materials are available. The physical properties of the expanded polystyrene used in this study are as follows; mass/unit volume = 25 kg/m^3, allowable compressible strength = 70 kPa, Young's modulus under triaxial compression at a confining pressure of 10 kPa = 2.5×10^4 kPa, and Poisson's ratio = 0.13. A large block of the expanded polystyrene material is provided and reduced to smaller blocks 1.0 m in width and 0.15 m in height. The length of the expanded polystyrene blocks, L_e, is varied from 0.1 m to 0.4 m according to the test conditions of each test.

Two types of geogrids are used in this study, and the physical properties are shown in Table 1. Some of the most important properties of geogrids under working stress conditions might be the secant tensile stiffness and aperture sizes. The difference in the tensile stiffness directly leads to a difference in the tensile shear stress induced along the geogrid layers, which subsequently contributes to a reduction in the lateral earth pressure on the wall. On the other hand, the aperture sizes, i.e. opening, determine the ratio of soil-against-soil contact area and

soil-against-geogrid contact area at the interface between geogrid layers and backfill materials, and therefore govern the dilative characteristics of the soil backfill, which subsequently affects the development of interface shear stresses between geogrid layers and backfill materials.

Test Procedures

In order to eliminate friction between model specimens and the walls of the model container, lubricant and vinyl sheets are used in this study. A silicon grease product is first applied to the entire surface of the walls. A vinyl sheet is then placed to cover each surface of the walls. The silicon grease is again applied and another set of vinyl sheets is placed. This technique to reduce friction is supported by Tatsuoka and Haibara (1985). They examined the shear resistance between Toyoura sand and smooth or lubricated surfaces, and demonstrated that the interface layers of the silicon grease, Teflon sheet, silicon grease and Teflon sheet reduce the interface friction angle to about 0.7° for a mean vertical stress of 30 kPa. Therefore, since the interface layers consisting of the silicon grease product and vinyl sheets used in this study are similar in style and in property to those examined by Tatsuoka and Haibara (1985), the interface friction angle between Toyoura sand and the walls of the model container in this study is considered to be negligibly small.

The model specimen is then prepared in the model container. Typically, soil layers of 0.15 m in height are placed on the floor and then on the top surface of the model specimen, before being tamped equally to achieve a designed relative density of $D_r = 75\%$. To monitor the soil density of each layer, a pair of cylindrically shaped small containers are placed on the top surface each time before pouring another layer of the soil material into the model container. These containers are pulled out and weighed to calculate the density of the model specimen. The expanded polystyrene blocks and geogrid layers are installed where necessary to produce the model configuration designed for each test. Care is especially taken between the expanded polystyrene blocks and the mobile retaining wall, where a thin layer of the soil materials is placed to avoid separation and to maintain contact between the expanded polystyrene blocks and the mobile retaining wall, which otherwise leads to erroneous measurement of lateral earth pressure.

When the entire model specimen is prepared, the rubber mattress is placed on the final top surface of the model specimen, and the model container is closed by the rigid lid. The rubber mattress is then air-inflated to apply a designed surcharge pressure to the model specimen. The following sequence of the surcharge pressure applications and wall movement is adopted in each test.

(1) The surcharge pressure is gradually increased at a rate of 10 kPa/min to achieve a prescribed surcharge pressure, q_o.
(2) The mobile retaining wall is activated to move laterally away from the model specimen at a rate of 0.05 mm/min, until the active stress state condition is achieved, (typically at a wall displacement of 4 mm).
(3) The surcharge pressure is gradually reduced.
(4) The mobile retaining wall is activated to move back to the original position at a rate of 0.15 mm/min.

The above procedure is repeated on the same model specimen under three different surcharge pressures, q_o, designed for each test. Since three cycles of surcharge loading, wall movement away from the soil specimen, surcharge unloading and wall movement back to the original position are employed on each model specimen, there can be some effects of the stress history on the measured data of earth pressures. However, it is believed in this study that the effects of stress history are minimal, since the wall movements towards the model retaining wall in between the successive cycles take place without surcharge pressures on top of the model specimen, and also a greater surcharge pressure is applied on the model specimen during a latter cycle than in previous cycles, which in turn could effectively eliminate the influence of stress history.

USE OF EXPANDED POLYSTYRENE BLOCKS BEHIND THE WALL

Figure 2 shows the installation patterns of the expanded polystyrene blocks adopted in test series A. In this test series, only the expanded polystyrene blocks are installed in the model specimens. In pattern E-1, which is adopted in tests A-1 to A-4, four pieces of the expanded polystyrene blocks are installed vertically behind the wall; however, the length of the expanded polystyrene blocks, L_e, is varied as 0.1, 0.2, 0.3 and 0.4 m in tests A-1 to A-4, respectively. In pattern E-2, which is adopted in test A-S, ten pieces of the expanded polystyrene blocks are installed in a step-like shape, and the length of the expanded polystyrene blocks, L_e, is fixed to 0.2 m. The details of test series A are summarized in Table 2, in which test O corresponds to an unreinforced model specimen, as was originally reported by Tsukamoto et al. (1999).

Figure 3 shows the stress path in the p-q plot for test A-1, where $p = (\sigma_v + \sigma_h)/2$, $q = (\sigma_v - \sigma_h)/2$, σ_v is the overburden stress at the depth of the earth pressure cells, and σ_h is the lateral earth pressure on the mobile retaining wall. It is informative and comprehensive to observe the stress path in the p-q plot. The stress point moves in a right-upward direction during surcharge loading, and reaches an at rest condition located on the K_o line. During the wall movement away from the model specimen, the stress point moves in a left-upward direction, and reaches an active stress state condition located on the K_a line. The stress point then moves in a left-downward direction during surcharge unloading, and finally moves in a right-downward direction during the wall movement back to the original position. Under three different surcharge pressures, the stress path experiences three different at rest conditions as well as three different active stress state conditions. By drawing up the straight lines on these three stress points based on the principle of the least

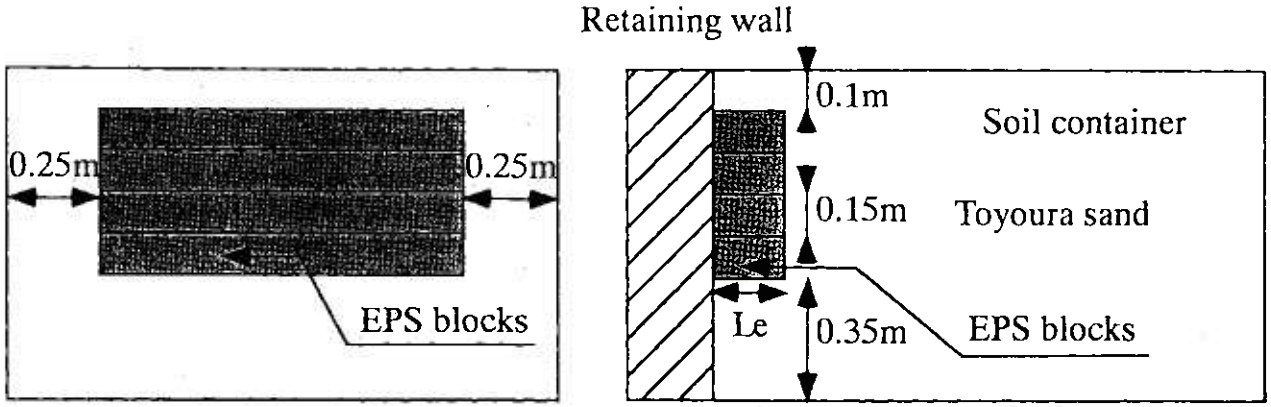

(a-1) View from front retaining wall (a-2) View from side wall

The length of EPS, Le, is varied as :
Le = 0.1m for Test A-1, Le = 0.2m for Test A-2,
Le = 0.3m for Test A-3, Le = 0.4m for Test A-4.

(a) Pattern E-1 (adopted in tests A-1 to A-4)

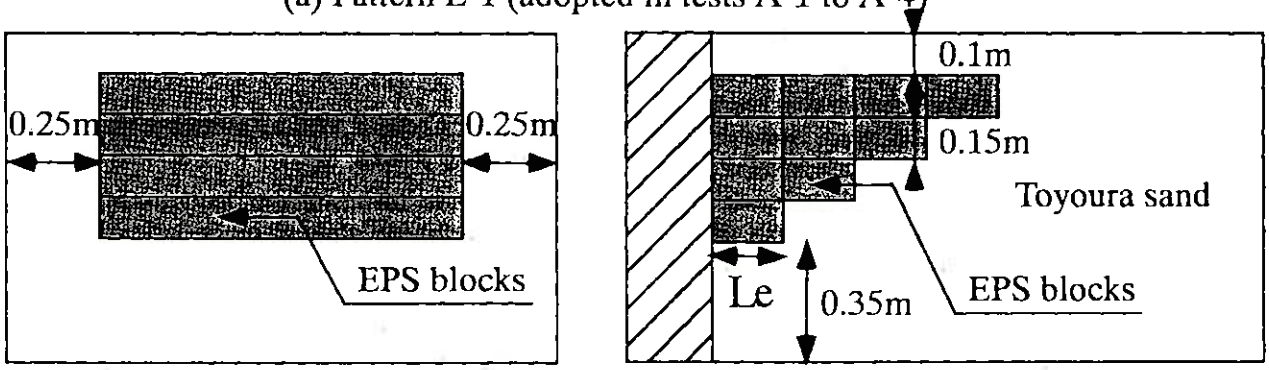

The length of EPS, Le, is 0.2m.

(b-1) View from front retaining wall (b-2) View from side wall

(b) Pattern E-2 (adopted in test A-S)

Fig. 2. EPS installation patterns in side view, (Test series A)

Table 2. Details of test series A and K_o and K_a values inferred from p-q plots

Test	D_r (%)	EPS blocks		q_o (kPa)	K_o	K_a	Remarks
		L_e (m)	Installation pattern				
O	75	—	unreinforced backfill	100, 200, 300	0.395	0.114	after Tsukamoto et al. (1999)
A-1	75	0.1	Pattern E-1	100, 150, 200	0.371	0.119	—
A-2	75	0.2	Pattern E-1	100, 150, 200	0.350	0.112	—
A-3	75	0.3	Pattern E-1	100, 150, 200	0.227	0.104	—
A-4	75	0.4	Pattern E-1	100, 150, 200	0.080	0.014	—
A-S	75	0.2	Pattern E-2	100, 150, 200	0.055	0.007	—

squares method, the coefficient of earth pressure at rest, K_o, and the coefficient of active earth pressure, K_a, can be inferred from the following equations,

$$K_o = \frac{\sigma_{ho}}{\sigma_v},\ K_a = \frac{\sigma_{ha}}{\sigma_v} \tag{1}$$

$$\left(\frac{q}{p}\right) = M_o = \frac{1-K_o}{1+K_o},\ \left(\frac{q}{p}\right)_a = M_a = \frac{1-K_a}{1+K_a} \tag{2}$$

where σ_{ho} and σ_{ha} are the lateral stresses at rest and at an active stress state on the mobile retaining wall, and M_o

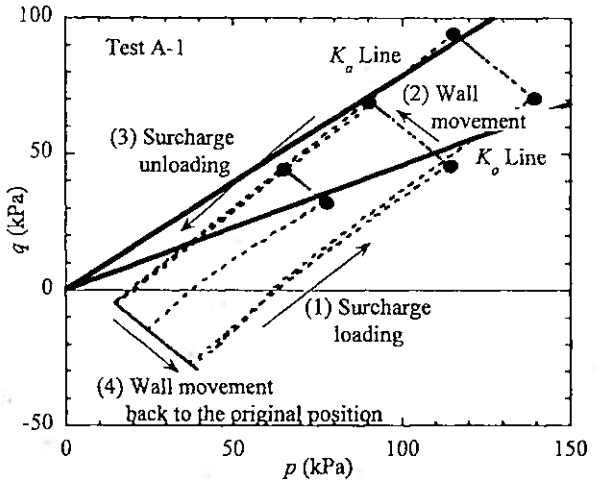

Fig. 3. Stress path in p-q plot, (Test A-1)

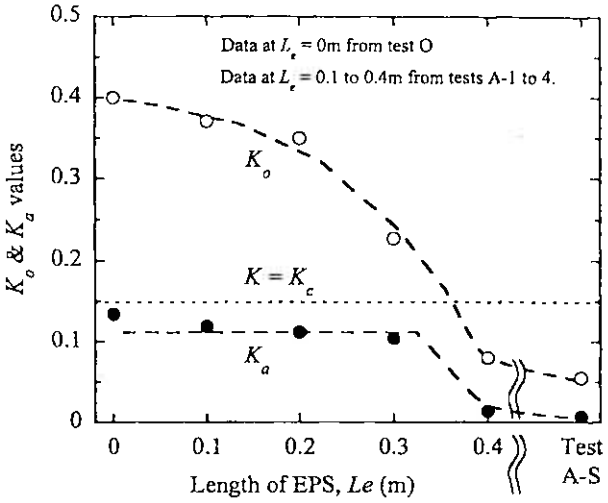

Fig. 5. K_o and K_a values against length of EPS blocks, L_e

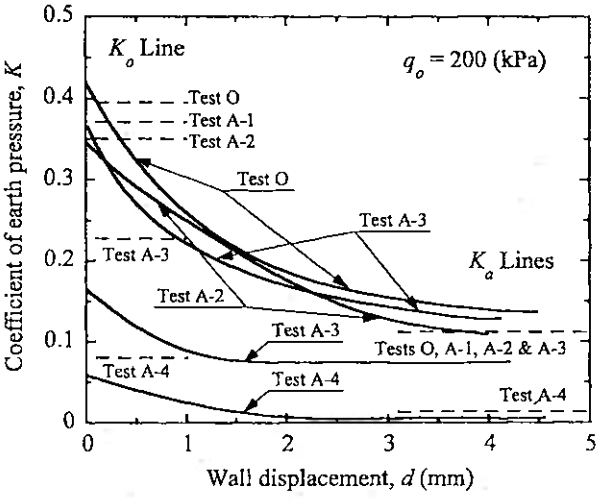

Fig. 4. Typical test results of K-d curves, (Test series A)

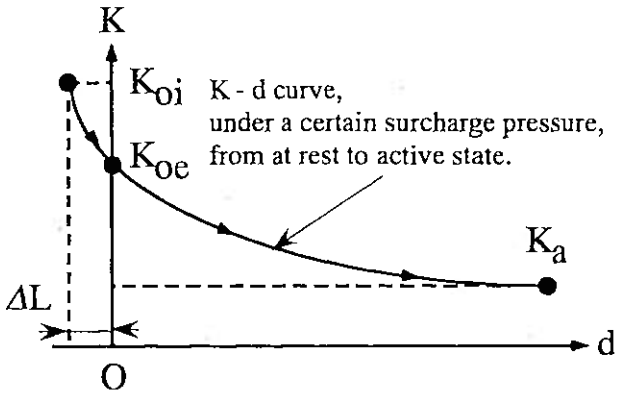

K_{oi} : coefficient of earth pressure at rest for unreinforced backfill

K_{oe} : coefficient of earth pressure at rest for backfill with EPS blocks

ΔL : compression of EPS blocks

Fig. 6. Interpretation of controlled yielding

and M_a are the inclinations of the K_o line and K_a line in the p-q plot, respectively. The K_o and K_a values thus inferred from the p-q plots are also shown in Table 2. Figure 4 shows typical test results of K-d curves for test series A, where K is the coefficient of earth pressure and d is the wall displacement away from the model specimens. In this diagram, the curves under the surcharge pressure q_o of 100 kPa for tests A-2, A-3 and A-4 are shown. The K_o and K_a values inferred from the p-q plot for each test are also shown. It is seen that the wall displacement necessary to move from the at rest to active stress state condition is typically about 4 mm. Figure 5 summarizes the K_o and K_a values inferred from the p-q plots plotted against the length of the expanded polystyrene blocks, L_e, employed in the tests. The data for $L_e = 0$ m correspond to the results of test O for the unreinforced model specimen. It is seen that the K_o value gradually reduces as the length of the expanded polystyrene blocks, L_e, increases, while the K_a value stays constant at $L_e = 0$ m up to 0.3 m; then these two values suddenly decrease at $L_e = 0.4$ m. In test A-S, the K_o and K_a values become even lower than in tests A-1 to A-4. The definition of the line, $K = K_c$, is explained later in this section.

It transpires that the inclusion of the expanded polystyrene blocks of up to 0.3 m in length scarcely affects the active earth pressure. Hence, it appears that only when the length of the expanded polystyrene blocks exceeds 0.4 m do the underweight expanded polystyrene blocks play a role in reducing the active earth pressure, in such a way that the solid underweight expanded polystyrene blocks replace part of the granular backfill behind the wall, which would have otherwise existed and caused plastic flow during the wall movement. It is evident that the active earth pressure for test A-S is the lowest among test series A, since the solid underweight expanded polystyrene blocks wholly replace the granular backfill which would have otherwise caused plastic flow behind the wall.

On the other hand, the reduction in the earth pressure

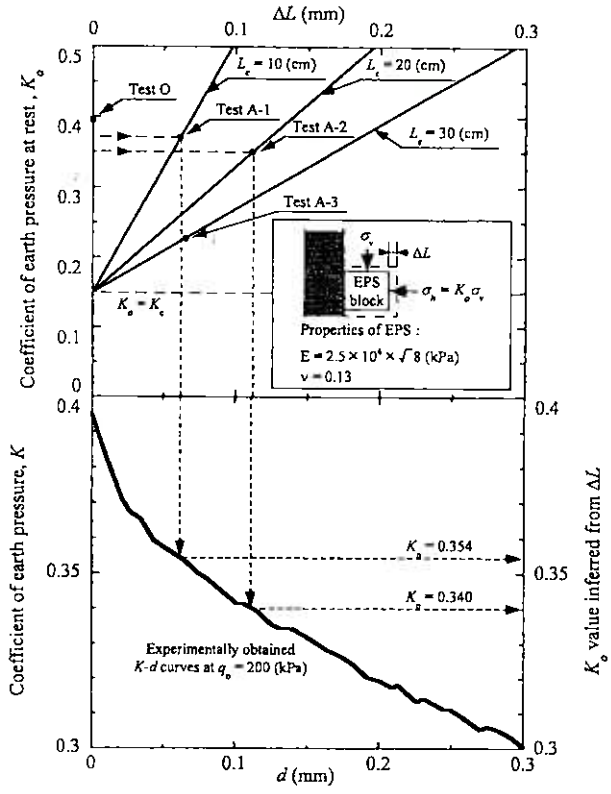

Fig. 7. Evaluation of reduction of earth pressure at rest due to controlled yielding

at rest with increasing length of expanded polystyrene blocks can be explained by the concept of controlled yielding, which was introduced by Karpurapu and Bathurst (1992). Herein, the role of compressible underweight expanded polystyrene blocks behind a rigid wall in the reduced earth pressure on the wall can be twofold, the controlled yielding resulting from compressibility of expanded polystyrene blocks and the reduced overburden pressure resulting from underweight expanded polystyrene blocks. It is stipulated in this study that under such higher confining pressures as conducted in the test series reported in this study, the role of controlled yielding due to compressibility of expanded polystyrene blocks becomes more predominant than the role of reduced overburden pressures due to underweight expanded polystyrene blocks. However, when the confining pressures were lower, the role of reduced overburden pressures due to underweight expanded polystyrene blocks would become more significant. Figure 6 demonstrates the interpretation of a controlled yielding concept with regard to the K-d curve of the retaining wall. Suppose the earth pressure at rest acting on a rigid wall is assumed to be K_{oi}. When a compressible layer such as expanded polystyrene blocks is installed behind the rigid retaining wall, the expanded polystyrene blocks are subjected to lateral compression. The soil adjacent to them is in turn caused to laterally expand in proportion to the lateral compression of the expanded polystyrene blocks, ΔL, and therefore the earth pressure decreases from K_{oi} to K_{oe}, as illustrated in Fig. 6. It is considered that the K_{oe} value demonstrated above is determined by the interference between the increase in the compressive stress on the expanded polystyrene blocks and the reduction in the lateral earth pressure exerted by the soil, i.e. nominally $(K_{oi}-K_{oe})\times\sigma_v$. Similar to the reduction of the active earth pressure shown in Fig. 5, it is conceivable that the earth pressure at rest significantly reduces due to the inclusion of underweight expanded polystyrene blocks of more than 0.4 m in length. The verification of the occurrence of controlled yielding in this study is illustrated in Fig. 7. As shown in the upper diagram, to obtain an initial estimate of the compressive displacement ΔL of a compressible layer such as expanded polystyrene blocks behind the wall, the following equation might be useful, which assumes an elastic deformation under a plane strain condition,

$$\Delta L=\varepsilon_h\times L_e, \tag{3}$$

$$\varepsilon_h=\frac{1+\nu}{E}\{(1-\nu)\sigma_h-\nu\sigma_v\}=\frac{1+\nu}{E}\sigma_v\{(1-\nu)K_o-\nu\}, \tag{4}$$

where ε_h, E, and ν are the lateral strain, Young's modulus, and Poisson's ratio of the expanded polystyrene blocks. Herein, the relation between K_o and ΔL is sensitive to the values of E and ν. Assuming in Fig. 7 that the elastic modulus of the expanded polystyrene E is related to the square root of the confining stress, and σ_h of about 80 kPa is expected under σ_v of 200 kPa, and since the modulus E at a confining pressure of 10 kPa is 2.5×10^4 kPa, as described above, it is assumed that $E=2.5\times10^4\times\sqrt{80/10}$ kPa. Equation (4) implies that it is only when $K_o>K_c=\nu/(1-\nu)$ that compressive strain occurs; otherwise extensional strain occurs. The lower diagram of Fig. 7 shows the K-d curves for the unreinforced model specimen, from which the reduced earth pressure at rest due to controlled yielding can be inferred, based on the compressive displacement ΔL obtained in the upper diagram. The K_o values thus inferred are 0.354 and 0.340 for tests A-1 and A-2, respectively, in comparison to the K_o values of 0.371 and 0.350, which are experimentally observed as shown in Table 2. It is also found that the concept of controlled yielding is applicable only for expanded polystyrene blocks of up to 20 cm in length.

USE OF GEOGRIDS WITHIN THE BACKFILL

Figure 8 shows the geogrid reinforcement patterns adopted in test series B. In this test series, only the geogrid layers are embedded within the model specimens, and are not tied to the back face of the model retaining wall. There are two types of geogrid, A and B, used in test series B. In pattern G-1, which is adopted in tests B-1, B-2 and B-4, three layers of the geogrid are embedded to a full length of the model container. In pattern G-2, which is adopted in tests B-3 and B-5, three layers of the geogrid are embedded at the same depths as in pattern A, but only, to half a length of the model container. Pattern G-3, which is adopted in test B-6, is similar to patterns G-1 and G-2 but with three layers of the geogrid embedded to one third of a full length of the model container.

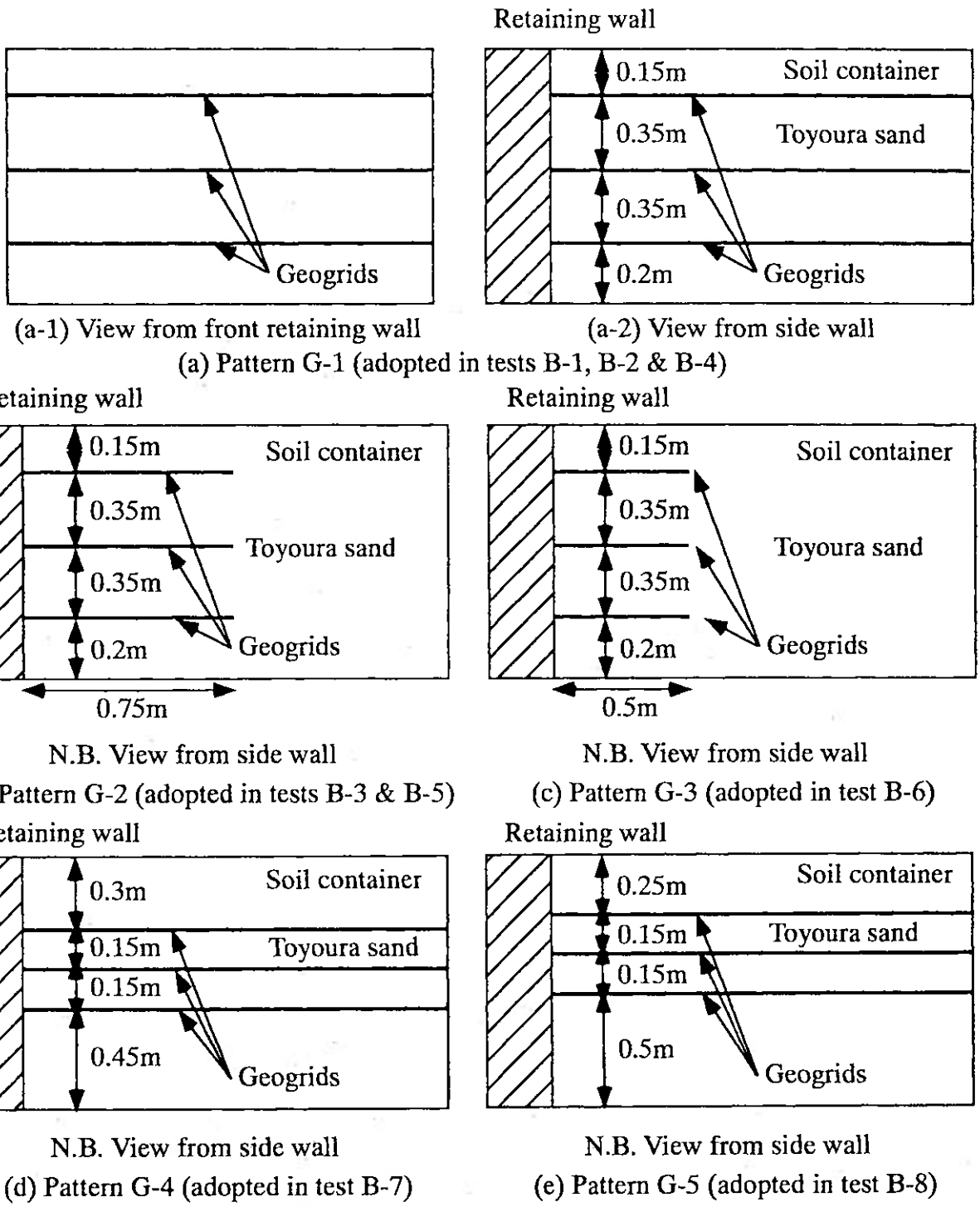

Fig. 8. Geogrid reinforcement patterns in side view, (Test series B)

Patterns G-4 and G-5, which are adopted in tests B-7 and B-8, respectively, also contain three layers of the geogrid embedded to a full length of the model container; however the depths of embedment are different from those for patterns G-1 to G-3. Patterns G-4 and G-5 are especially designed to make a comparison with the results from test series C, which used the expanded polystyrene blocks as well as the geogrid. The details of test series B are summarized in Table 3. It should be noted that some of the test results, i.e. tests B-1, B-3, B-4 and B-7, were originally reported by Tsukamoto et al. (1999, 2001).

Figure 9 shows the stress path in the p-q plot for test B-7. Test series B is found to experience stress paths similar to test series A, and allow K_o and K_a lines to be drawn in the p-q plots. The K_o and K_a values thus inferred from the p-q plots, based on Eqs. (1) and (2), are also indicated in Table 3. Figure 10 shows the K_o and K_a values plotted against the test code, i.e. O, B-1 to B-8. The earth pressures at rest for geogrid reinforced model specimens appear to be the same as that for the unreinforced model

Table 3. Details of test series B and K_0 and K_a values inferred from p-q plots

Test	D_r (%)	Geogrids		q_0 (kPa)	K_0	K_a	Remarks
		Type	Reinforcement pattern				
O	75	—	Unreinforced backfill	100, 200, 300	0.395	0.114	after Tsukamoto et al. (1999)
B-1	75	A	Pattern G-1	100, 200, 300	0.411	0.048	after Tsukamoto et al. (1999)
B-2	75	A	Pattern G-1	100, 150, 200	0.438	0.064	—
B-3	75	A	Pattern G-2	100, 200, 300	0.401	0.045	after Tsukamoto et al. (1999)
B-4	75	B	Pattern G-1	100, 200, 300	0.403	0.076	after Tsukamoto et al. (1999)
B-5	75	B	Pattern G-2	100, 150, 200	0.462	0.063	—
B-6	75	B	Pattern G-3	100, 150, 200	0.476	0.085	—
B-7	75	B	Pattern G-4	100, 150, 200	0.403	0.076	after Tsukamoto et al. (2001)
B-8	75	B	Pattern G-5	100, 150, 200	0.397	0.095	—

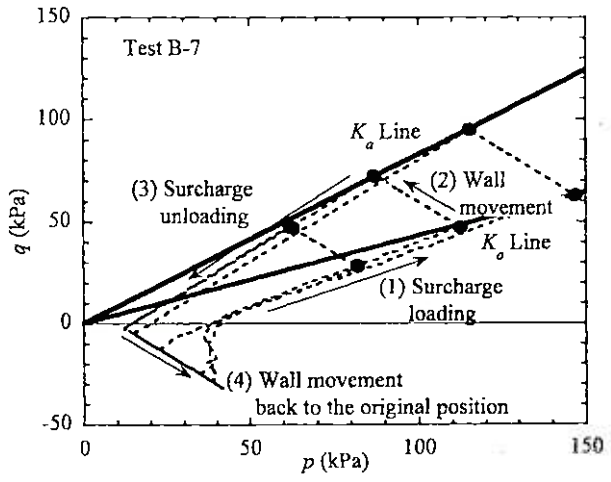

Fig. 9. Stress path in p-q plot, (Test B-7)

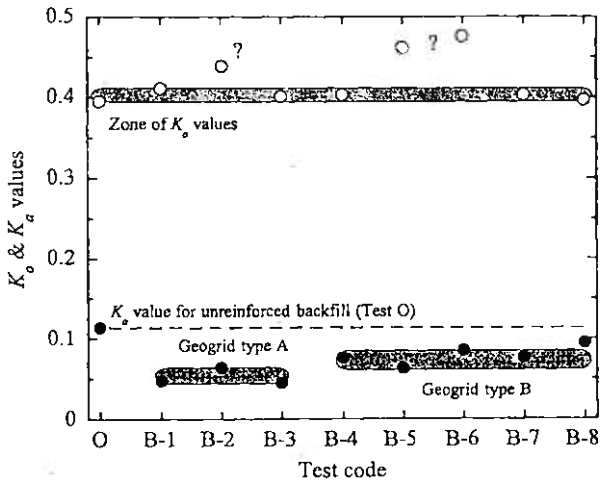

Fig. 10. K_0 and K_a values of test series B

specimen and to stay almost constant, except for erroneously higher values exhibited by some data. On the other hand, the active earth pressures for geogrid reinforced model specimens are found to be lower than that for the unreinforced model specimen. In the authors' opinion, the at-rest conditions have more tendency to accumulate the influence of stress path history experienced during successive cycles of wall movement under three different surcharge pressures applied on the same model specimens, which initially results from subtle differences in the operators' handling of initial preparation of model specimens. On the other hand, the active stress state conditions tend to be free from subtle differences in the operators' handling. It is partly explained by the fact that a K_a line in the p-q plot resembles a steady state envelope defined for sand (Ishihara, 1993), in which a steady state is independent of initial deposition of soils. From the results shown in Fig. 10, it is envisaged that the active earth pressure seems to be dependent on the type of geogrid. It was discussed above that among the properties of geogrids, there are two factors that effectively contribute to the reinforcement mechanism under working stress conditions: tensile stiffness and aperture size. However, it is still not feasible to discuss how these two factors affect the active earth pressure from the test results reported in this study.

Figures 11 and 12 show the K-d curves for test O of the unreinforced model specimen and for test B-3 of the geogrid-reinforced model specimen, under three different surcharge pressures, $q_0 = 100$, 200, 300 kPa, respectively. It is seen that the wall displacements necessary to reach active stress state conditions are greater under larger surcharge pressures for the geogrid-reinforced model specimens as well as for the unreinforced model specimen.

In test series B, as well as in test series C described below, geogrid layers embedded within the model specimens are instrumented with electrical resistance strain gauges at several equally spaced positions, to measure the tensile strains induced along the layers of the geogrid. Care is taken here with the difference between the tensile strains measured by strain gauges and the true global strains, as reported by Perkins and Lapeyre (1997). It is demonstrated that the tensile strains measured by strain gauges are local values, and do not represent the average

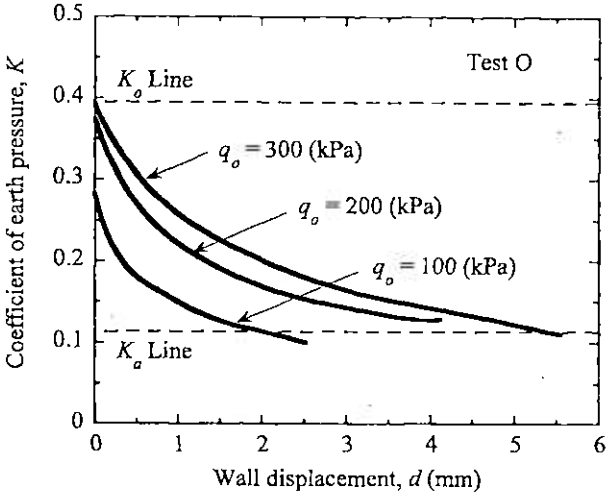

Fig. 11. *K-d* curves of test O, (after Tsukamoto et al. (1999))

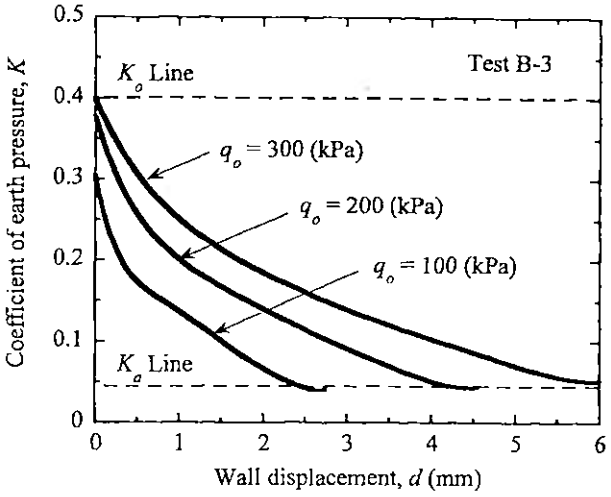

Fig. 12. *K-d* curves of test B-3

strains (global strains) over a much greater length between the strain-gauged points along the geogrids. Therefore, in this study, the tensile strains measured by strain gauges are converted to true global strains, based on independently conducted tension tests. The outcome of the geogrid tensile strain measurement for test series B will be discussed below in comparison with the results of test series C. Some aspects of the geogrid tensile strains and interface shear stresses are illustrated in Appendix, in relation to the reduced active earth pressures of geogrid reinforced model specimens.

COMBINED USE OF EXPANDED POLYSTYRENE BLOCKS AND GEOGRIDS

Figure 13 shows the reinforcement patterns adopted in test series C. In this test series, the expanded polystyrene blocks as well as geogrid layers are installed in the model specimens. In pattern EG-1, which is adopted in test C-1, four of the expanded polystyrene blocks of 0.2 m in length are installed vertically behind the wall, and three layers of the geogrid are embedded within the model specimen with their ends tightly fixed between two adjacent expanded polystyrene blocks. Pattern EG-2, which is adopted in test C-2, is similar in reinforcement pattern to pattern EG-1, except for some differences in the depths of embedment of the expanded polystyrene blocks and geogrid layers. The details of test series C are summarized in Table 4.

Figure 14 shows the stress path in the *p-q* plot for test C-1. It is seen that test series C also follows stress paths similar to test series B and C, and there are K_o and K_a lines in the *p-q* plots. The K_o and K_a values thus obtained from the *p-q* plots are also indicated in Table 4. With respect to the similarity in reinforcement patterns, test C-1 reinforced with the expanded polystyrene blocks and geogrid layers can be compared with test B-7 reinforced only with geogrid layers. Similarly, test C-2 can be compared with test B-8. It is found that the K_o value for test C-2 is almost identical to that for test A-2. However, the K_o value for test C-1 is unexpectedly lower than those for tests A-2 and C-2, which in the authors' opinion might be related to the operators' handling of the model specimen with a complex model configuration in which expanded polystyrene blocks as well as geogrid layers are involved. It can be concluded that the K_o value for test series C is also governed by a controlled yielding concept. It is also found that the active earth pressure for test C-1 (C-2) is lower than that for test B-7 (B-8). It was concluded above from the results of test series A that the inclusion of 0.2 m long expanded polystyrene blocks scarcely alters the active earth pressure. From that point of view, the difference of the active earth pressures between test series B and C might have come from additional benefits resulting from the fixity between the expanded polystyrene blocks and geogrid layers, and also from the expanded polystyrene blocks acting as a facing unit against a rigid wall. Figures 15 and 16 compare the distributions of geogrid tensile strains induced along the geogrid layers for tests B-7 and C-1, and tests B-8 and C-2, respectively. For tests B-7 and B-8, in which the geogrid layers are not tied at each end, the geogrid tensile strains at each free end are assumed to be zero. However for tests C-1 and C-2, since the geogrid layers are fixed between two adjacent expanded polystyrene blocks, the tensile strains at the fixed points are allowed to grow, as shown in Figs. 15 and 16. It is found that overall, the geogrid tensile strains for tests C-1 and C-2 are greater than those for tests B-7 and B-8, respectively. It is considered that the difference in the geogrid tensile strains induced along the geogrid layers partly contributes to the reduction in the active earth pressure, where the larger geogrid tensile strains lead to a greater reduction in the active earth pressure. The physical interpretation of the geogrid tensile strains, geogrid interface shear stresses, and reduction in the active earth pressure is described in the Appendix. Based on the principle described there, the values of ΔK and K_g are plotted against wall displacement d, for tests B-7 and C-1, in which $\Delta K = K_{au} - K_{ar}$, (Appendix), as shown in Fig. 17. It is found that when it comes to comparison of the K_g values,

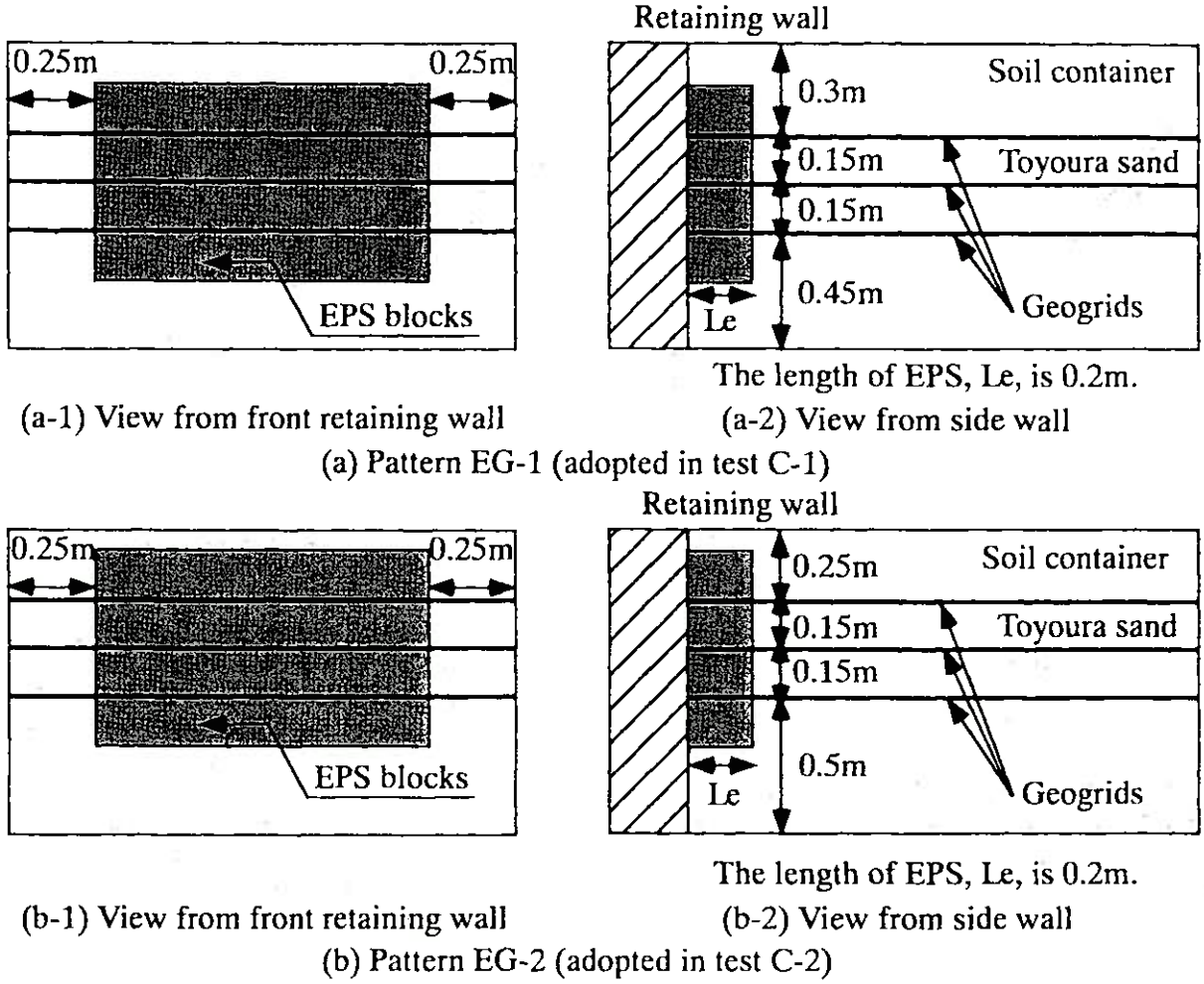

Fig. 13. Reinforcement patterns in side view, (Test series C)

Table 4. Details of test series C and K_o and K_a values inferred from p-q plots

Test	D_r (%)	EPS blocks		Geogrids		q_o (kPa)	K_o	K_a	Remarks
		L_e (m)	Installation pattern	Type	Reinforcement pattern				
O	75	—	Unreinforced backfill	—	—	100, 200, 300	0.395	0.114	after Tsukamoto et al. (1999)
C-1	75	0.2	Pattern EG-1	B	Pattern EG-1	100, 150, 200	0.292	0.042	after Tsukamoto et al. (2001)
C-2	75	0.2	Pattern EG-2	B	Pattern EG-2	100, 150, 200	0.350	0.070	—

the difference between tests B-7 and C-1 is relatively small. In comparison of the ΔK and K_g values, it was observed by Tsukamoto et al. (1999) that the ΔK value tends to become greater than the K_g value for the dense model granular backfill reinforced with geogrid layers. However, it appears in this test that the ΔK value tends to become identical to the K_g value, although the ΔK value for test B-7 behaves in an erroneous manner at a wall displacement, d, smaller than 2 mm, which might support the assumption that the tensile strains induced along geogrid layers contribute to the reduction in the active earth pressure. The ΔK value for test C-1 at a small wall displacement, d, is large due to controlled yielding, and tends to subside, and then rise again, which might be related to the effect of the expanded polystyrene blocks acting as a facing unit. Figure 18 schematically illustrates the influence of various factors on the reduction in the earth pressure developed with a wall movement.

SUMMARY OF EXPERIMENTAL FINDINGS

From the perspective of the test results obtained in test series A, B and C, described above, the following summary of the experimental findings can be made.

(1) The inclusion of a compressible layer such as expanded polystyrene blocks behind a rigid wall is capable of reducing the earth pressure at rest, in comparison to an unreinforced model specimen. This can be explained by a controlled yielding concept. However, the expanded polystyrene blocks

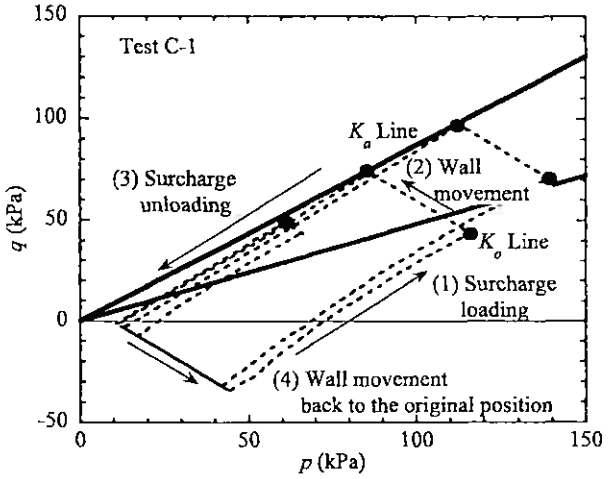

Fig. 14. Stress path in p-q plot, (Test C-1)

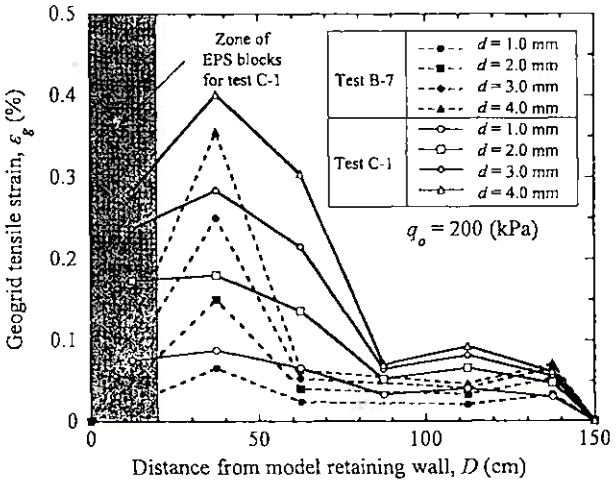

Fig. 15. Distributions of geogrid tensile strain, (Tests B-7 and C-1)

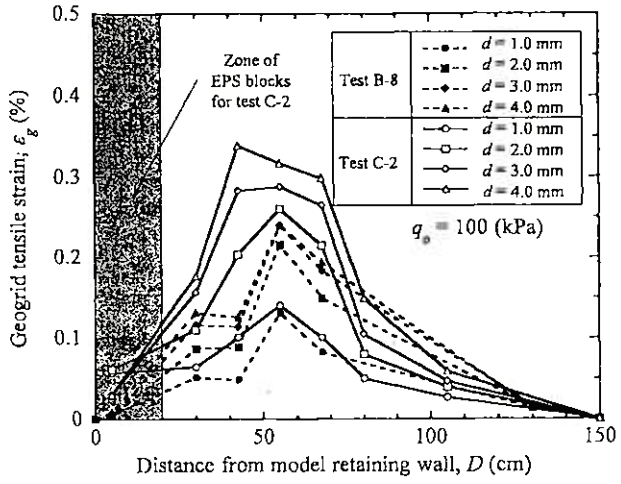

Fig. 16. Distributions of geogrid tensile strain, (Test B-8 and C-2)

inclusion scarcely alters the active earth pressure unless the length of the expanded polystyrene blocks is large enough.

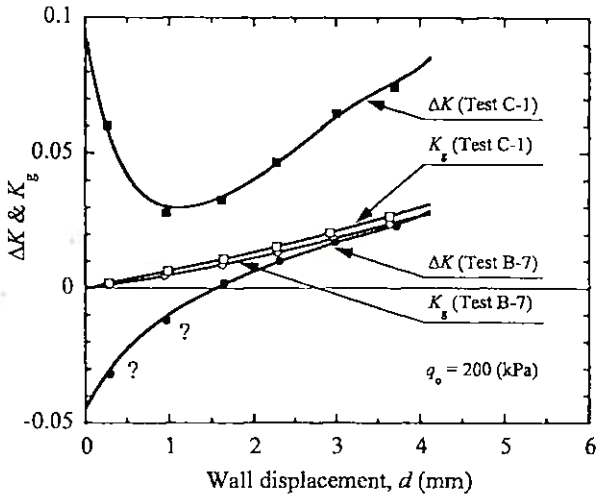

Fig. 17. ΔK and K_g-d curves, (Test B-7 and C-1)

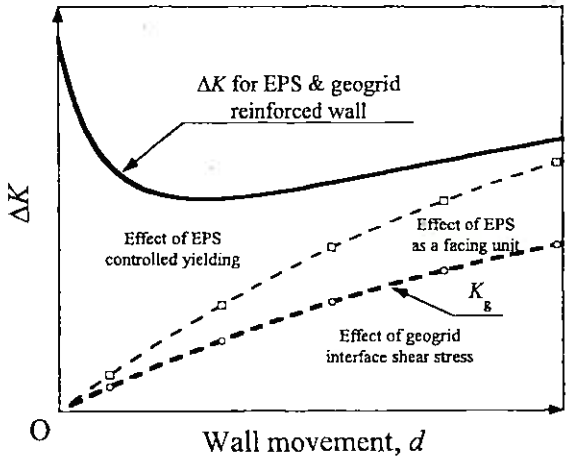

Fig. 18. Interpretation of ΔK and K_g-d curves

(2) The layers of geogrid embedded within model specimens scarcely alter the earth pressure at rest, in comparison to an unreinforced model specimen; however, they are capable of reducing the active earth pressure. The reduction in the active earth pressure can be related to tensile strains induced along the geogrid layers.

(3) The combined use of expanded polystyrene blocks and geogrid layers is capable of reducing the earth pressure at rest, as well as the active earth pressure. The reduction in the earth pressure at rest can be demonstrated by a controlled yielding concept due to compression of expanded polystyrene blocks. The reduction in the active earth pressure can be related to tensile strains induced along the geogrid layers and also to the fixity between the expanded polystyrene blocks and the geogrid layers.

PRACTICAL CONSIDERATIONS

In this study, the inclusion of a compressible layer such

as expanded polystyrene blocks behind a rigid wall, and geogrid layers embedded within a dense granular backfill were examined as an earth reinforcement technique for retaining wall structures. It was illustrated that the inclusion of a compressible layer behind rigid earth retaining structures achieves controlled yielding of soils behind rigid walls and reduces the earth pressure at rest. On the other hand, the embedment of geogrid layers reduces the active earth pressure due to tensile strains induced along geogrid layers. This reinforcement technique might be useful in increasing the stability of rigid walls retaining granular backfills sitting on relatively steep slopes, where slope instability might be anticipated. However, to put this reinforcement technique into practical use, careful consideration is necessary: the advantages of usage of the expanded polystyrene and geogrid materials have been highlighted, but the downsides of their usage, such as fragility, buoyancy and endurance and degradation characteristics of the expanded polystyrene and geogrid materials, have been ignored. Because of the fragile characteristics of the expanded polystyrene materials, the problems of fatigue at fixed positions between the expanded polystyrene blocks and geogrid layers, and of installation damage need to be carefully examined. Because of the buoyant characteristics of the expanded polystyrene materials, a proper drainage system needs to be designed for this particular structure. A design life span of this structure needs to consider various endurance and degradation characteristics of the expanded polystyrene and geogrid materials (Koerner, 1994; among others). It is noted here that any layer of compressible geosynthetic materials which is capable of inducing the occurrence of controlled yielding may be able to replace the expanded polystyrene blocks examined in this study.

CONCLUSIONS

As one of the reinforcement techniques for retaining wall structures, the inclusion of a compressible layer such as expanded polystyrene blocks behind a rigid wall and geogrid layers embedded within a dense granular backfill were examined using a mobile model retaining wall. The coefficients of earth pressure at rest and active earth pressure were especially examined. The role of the compressible expanded polystyrene blocks was interpreted by a controlled yielding concept, which contributes to the reduction in the earth pressure at rest. The role of the geogrid layers was discussed in relation to geogrid tensile strains, which contributes to the reduction in the active earth pressure. The combined use of the expanded polystyrene blocks and geogrid layers provides fixity between the expanded polystyrene blocks and geogrid layers, and a facing unit consisting of the expanded polystyrene blocks against a rigid wall, which contributes to the even greater reduction in the active earth pressure. This reinforcement technique can be practically viable to prevent instability of rigid walls retaining granular backfills sitting on relatively steep slopes.

ACKNOWLEDGEMENTS

This study is the outcome of the past six years of research carried out by the soil mechanics group at the Tokyo University of Science. The authors would like to acknowledge the past and current students, Messrs H. Aoki, K. Kinugasa, H. Wakayama, K. Irie, Y. Ogura, S. Furuta, R. Hashimoto, Y. Okada, R. Yamazaki, T. Tsurumaki, T. Kanno and M. Takagishi, who made great efforts for the model tests reported in this study. Thanks are also extended to Dr. T. Saitoh, Mr. K. Hara, and the staff at the Technical Research Institute of Mitsui Construction Co., Ltd., where permission to locate the test apparatus was granted. The first author would like to thank the Ogawa Foundation for providing him with financial assistance.

NOTATION

d: wall displacement away from model specimens
$l_{i,i+1}$: length between adjacent strain gauged points i and $i+1$
l_{TP}: transition point of geogrid interface shear stress changing from positive to negative along the l-coordinate
p: two-dimensional mean stress, $=(\sigma_v+\sigma_h)/2$
q: two-dimensional shear stress, $=(\sigma_v-\sigma_h)/2$
q_o: surcharge pressure
B: width of retaining wall
E: Young's modulus of expanded polystyrene blocks
H: effective height of retaining wall reinforced by a single geogrid layer
K: coefficient of earth pressure
K_g: $=\sigma_{hg}/\sigma_v$
K_{oc}: imaginary coefficient of earth pressure at rest on retaining wall with expanded polystyrene blocks
K_{oi}: imaginary coefficient of earth pressure at rest on rigid retaining wall
K_{ar}: coefficient of active earth pressure for geogrid reinforced model specimen
K_{au}: coefficient of active earth pressure for unreinforced model specimen
ΔK: $=K_{au}-K_{ar}$, reduction in the earth pressure due to reinforcement
L: aperture size (length) of geogrids
L: length of a geogrid layer
L_e: length of expanded polystyrene blocks
ΔL: lateral compression of expanded polystyrene blocks
M_a: inclination of K_a line in p-q plot
M_o: inclination of K_o line in p-q plot
T_i: geogrid tensile force per unit width at point i
T_{max}: maximum tensile force per unit width
W: aperture size (width) of geogrids
ε_f: geogrid tensile strain at failure
ε_g: geogrid tensile strain
ε_h: lateral compressive strain of expanded polystyrene blocks
ν: Poisson's ratio of expanded polystyrene blocks
σ_h: lateral earth pressure on model retaining wall
σ_{hg}: apparent lateral stress sustained by a geogrid layer
σ_{ha}: lateral active earth pressure on model retaining wall
σ_{ho}: lateral earth pressure at rest on model retaining wall
σ_v: overburden stress at depth of earth pressure cells
τ_i: geogrid interface shear stress at the midpoint between points i and $i+1$
τ: geogrid interface shear stress

REFERENCES

1) Ishihara, K. (1993): *Liquefaction and flow failure during earthquakes*, *Géotechnique*, **43** (3), 351–415.
2) Karpurapu, R. and Bathurst, R. J. (1992): Numerical investigation of controlled yielding of soil-retaining wall structures, *Geotextiles and Geomembranes*, **11**, 115–131.
3) Koerner, R. M. (1994): Designing with geosynthetics, Prentice Hall.
4) Partos, A. M. and Kazaniwsky, P. M. (1987): Geoboard reduces lateral earth pressures, *Proc. of Geosynthetics'87 Conf.*, New Orleans, USA, 628–639.
5) Perkins, S. W. and Lapeyre, J. A. (1997): In-isolation strain measurement of geosynthetics in wide-width strip tension test, *Geosynthetics Int.*, **4** (1), 11–32.
6) Tatsuoka, F. and Haibara, O. (1985): Shear resistance between sand and smooth or lubricated surfaces, *Soils and Foundations*, **25** (1), 89–98.
7) Tsukamoto, Y., Ishihara, K., Higuchi, T. and Aoki, H. (1999): Influence of geogrid reinforcement on lateral earth pressures against model retaining walls, *Geosynthetics Int.*, **6** (3), 195–218.
8) Tsukamoto, Y., Ishihara, K., Nakazawa, H., Kon, H., Masuo, T. and Hara, K. (2001): Combined reinforcement by means of EPS blocks and geogrids for retaining wall structures, Landmarks in Earth Reinforcement, *Proc. of International Symposium on Earth Reinforcement* (ed. by Ochiai, Otani, Yasufuku and Omine), 483–487.

APPENDIX: EVALUATION OF GEOGRID INTERFACE SHEAR STRESSES

Some aspects of geogrid tensile strains and geogrid interface shear stresses are illustrated, in relation to active earth pressure on a rigid retaining wall. The role of the geogrid interface shear stresses on the reduced active earth pressure is especially highlighted. The details of the following discussion, based on the model test results, are given by Tsukamoto et al. (1999).

Suppose the geogrid tensile strains are induced along a geogrid layer as shown in Fig. A-1. It is noted here that the tensile strain measured by a strain gauge needs to be converted to the true global strain, which represents the average strain over the length of two adjacent strain gauged points (Perkins and Lapeyre, 1997; among others). The geogrid tensile force, T_i, per unit width at point i from the wall can be calculated from the independently conducted tension tests, as shown in Fig. A-1.

The distribution of the geogrid interface shear stresses, τ_i, induced along a geogrid layer can be calculated as follows,

$$\tau_i = \frac{T_{i+1} - T_i}{2l_{i,i+1}} \tag{A-1}$$

where τ_i is the geogrid interface shear stress at the midpoint between points i and $i+1$, and $l_{i,i+1}$ is the length between adjacent strain gauged points. The geogrid interface shear stresses are supposed to develop on both sides of a geogrid layer. A transition point exists, where the geogrid interface shear stress changes from positive to negative values. It is clear that this transition point is equivalent to the point where the maximum tensile force, T_{max}, is located, and the following equation holds true,

$$T_{max} = -2\int_{l_{TP}}^{L} \tau dl \tag{A-2}$$

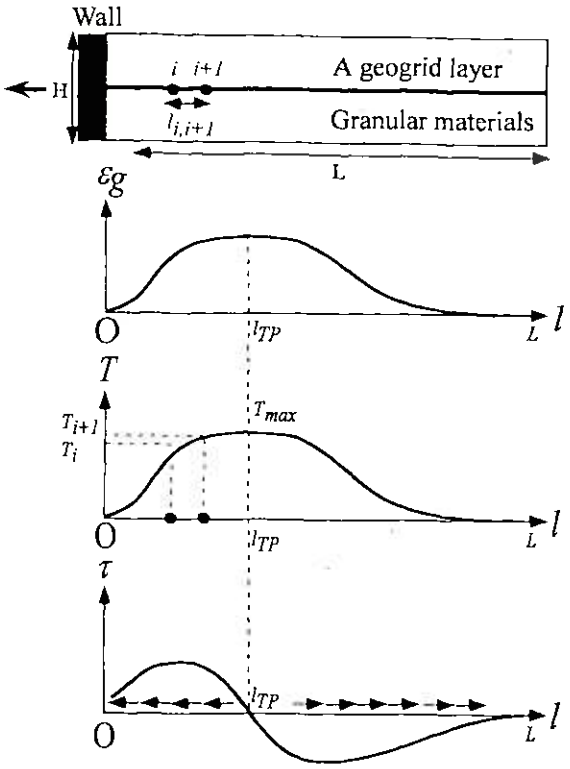

Fig. A-1. Schematic illustration of geogrid tensile strain, tensile force, and interface shear stress induced along geogrid layer

where T_{max} is the maximum tensile force per unit width, τ is the interface shear stress distributed along a geogrid layer, l_{TP} is the transition point along the l-coordinate, and L is the entire length of a geogrid layer. This implies that the geogrid interface shear stress induced between the retaining wall and the transition point acts towards the wall, while the geogrid interface shear stress induced between the transition point and far beyond acts away from the wall. Therefore, when the soil resistance is mobilized during the wall movement, the geogrid interface shear stress induced behind the transition point effectively pulls back the backfill away from the wall, and contributes to the reduced active earth pressure on the wall. It is also noteworthy that it is at this transition point that the development of a potential sliding surface is imposed within the plastically deformed backfill.

The apparent lateral stress, σ_{hg}, sustained by a geogrid layer, which acts normal to the retaining wall, is then defined as follows,

$$\sigma_{hg} = \frac{T_{max}B}{HB} \tag{A-3}$$

where B is the width of the retaining wall and a geogrid layer, and H is the effective reinforced height of the wall covered by a single geogrid layer. As an initial estimate of the reduced active earth pressure, the following equation might be useful,

$$K_{ar} = K_{au} - K_g \tag{A-4}$$

where K_{ar} and K_{au} are the active earth pressures for a geogrid reinforced backfill and for an unreinforced backfill, respectively, and $K_g = \sigma_{hg}/\sigma_v$.